HARDMEKO 2004
Hardness Measurements Theory and Application in Laboratories and Industries
11-12 November, 2004, Washington, D.C., USA

NANO-INDENTATION TESTING ON IN SITU MECHANICAL PROPERTIES OF ADHESIVES

Masayuki FUJITSUKA, Chiaki SATO

Precision and Intelligence Laboratory, Tokyo Institute of Technology, Kanagawa, JAPAN

Abstract – The mechanical properties of adhesives are determined either from bulk material samples from adhesively bonded joints. For many years there has been controversy as to whether the mechanical properties obtained through testing bulk material are representative of the adhesive in its thin-film form. The use of adhesive bonding as a method of joining structural members in advanced structures is increasing. A major advantage of adhesive bonding is that it enables dissimilar materials to be joined and reduces the localized stresses encountered when using mechanical fastening such as bolts and rivets. In design process it is important to know unambiguously the mechanical properties of the materials being used. Because the adhesive is used in thin-film from, to obtain the mechanical characteristics of the adhesive in situ is hoped.

In several papers it has been found that the adhesive material has different mechanical properties when tested in the thin-film form and bulk form, and further that a thickness effect exists, causing the properties to depend on the thickness of the bondline. However, the good agreement between thin-film and bulk properties is obtained in other papers. Moreover, the existence of the boundary layer in the adhesive layer is reported.

In this paper, nano-indentation testing is carried out for the calibration specimens and two kinds of the specimens of adhesive. And the method in the former paper applied to know the distribution of local mechanical properties in the adhesive layers and the bulk material.

Keywords: Mechanical Properties of Adhesives, Expanded Nano-indentation Theory, Practical Adhesion

1. INTRODUCTION

The main problem in characterizing an adhesive as a structural material is to determine whether its behaviour in a confined state differs from that of its bulk material reference. Solution of this problem is essential for an evaluation of design allowable of bonded joints. In several papers[1] it has been found that the adhesive material has different mechanical properties when tested in the thin-film form and bulk form, and further that a thickness effect exists, causing the properties to depend on the thickness of the bondline. However, the good agreement between thin-film and bulk properties is obtained in other papers[2]. Moreover, the existence of the boundary layer in the adhesive layer is reported. In design process it is important to know unambiguously the mechanical properties of the materials being used. Because the adhesive is used in thin-film from, to obtain the mechanical characteristics of the adhesive in situ is hoped. Nano-indentation testing is elaborate and precise measurement to obtain the distribution of local mechanical properties. The aim of this study is to determine the in situ material properties of adhesive by the expanded nano-indentation theory proposed in the former paper[3].

2. EXPERIMENTS

2.1 Nano-indentation tester

Experiments were carried out using the Fischer scope H100C tester made by Helmut Fischer GmbH + Co. KG. Germany. Specifications of the tester are as follows: the load range is 0.4mN to 1N, the displacement range is 0 to 700μm, and the displacement resolution is 0.2nm. The passive vibration isolator using magnet and α-gel has been set under the tester so as to exclude the vibration noise enough.

2.2 Specimens and the indenter

The Specimens used in the nano-indentation test are listed in Table 1. The HMV500 specimen (the standard blocks for hardness made by Yamamoto Scientific Tool Laboratory Co.LTD. Japan) and the BK7 specimen (glass specimen made by Kadomi Optical Industry) are used as the calibration specimens. The specimen of the adhesive prepared two kinds (the bulk specimen and the specimen to which two aluminum alloy plates were sticked with adhesive [Fig.1]). The adhesive used was bisphenol A type epoxy prepolymer (Epikote 828, Japan Epoxy Resin Co.LTD. JAPAN). The curing agent was ATU based epoxy hardner (Epomate B002, Japan Epoxy Resin Co.LTD. JAPAN). The ratio of epoxy prepolymer and curing agent is 2:1.

The indenter used is the diamond quadrangular pyramidal indenter, namely Vickers indenter, having the opposed face angle β_{Qua} =136° and the opposed edge angle γ_{Qua}=148.1°. Young's modulus and Poisson's ratio of the indenter are supposed in as follows: E_I=1140GPa, μ_I=0.07[4]. Therefore, $I(E)$ has the value 8.73×10^{-4}GPa^{-1} and the values of E_S for the specimens and $F(E)_{IS}$ are listed in Table 1. [μ_S=0.3 is assumed for the metal specimens]

Table 1 Specifications of the specimens

No.	Symbol	Hardness value of standard blocks for hardness	JIS code	Composition	Young's modulus E_S [GPa]	Poisson's Ratio μ_S	$S(E)$ [GPa^{-1}]	$F(E)_{IS} = I(E) + S(E)$ [GPa^{-1}]
1	BK7	-	-	B_2O_3-SiO_2	79.2	0.214	12.1×10^{-3}	12.9×10^{-3}
2	HMV500	HMV 499(98mN)	SK5	Carbon Steel	210	0.3	4.33×10^{-3}	5.21×10^{-3}
3	Adhesive	-	-	Epoxy Resin	2.06	0.38	0.42×10^{-2}	1.30×10^{-3}

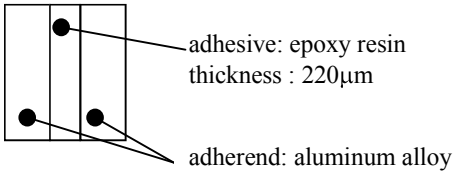

Fig.1. Schematic figure of specimen

2.3 Experimental results

The experimental data of the loading and unloading curves are shown in Fig.2–Fig.4. In Table 2, the indentation depth δ_t and elastic recovery displacement δ_r for the BK7 specimen and the HMV500 specimen used as the calibration specimens and the bulk specimen are listed. In Table 3, the averages of the measured values for the specimen to which two aluminum alloy plates were sticked with adhesive are listed.

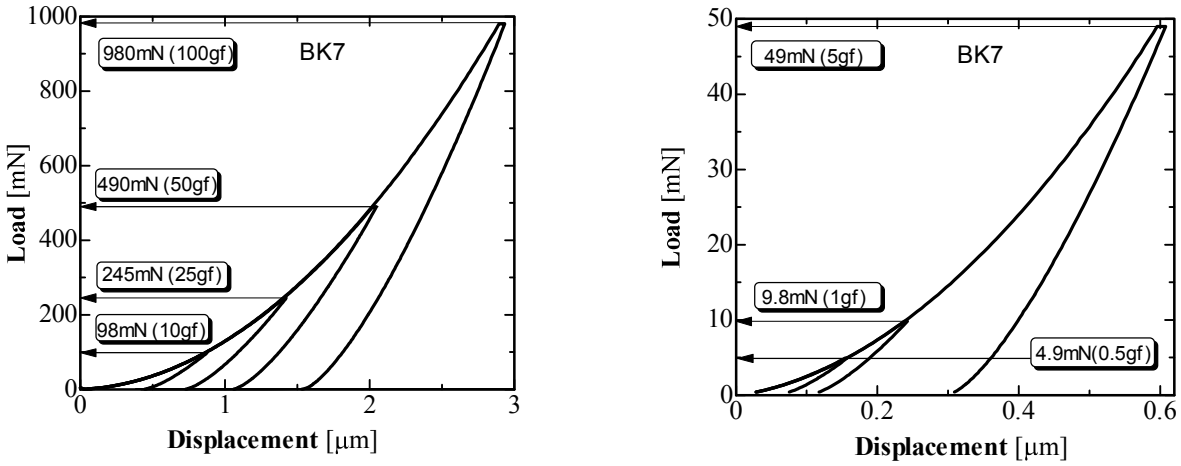

Fig.2 Experimental data of loading and unloading curves for BK7 specimen

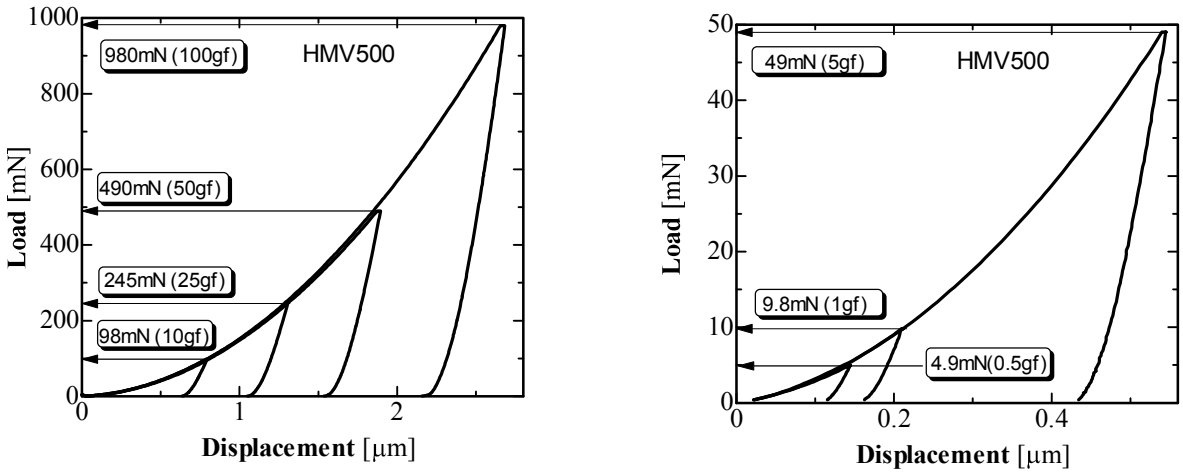

Fig.3 Experimental data of loading and unloading curves for HMV500 specimen

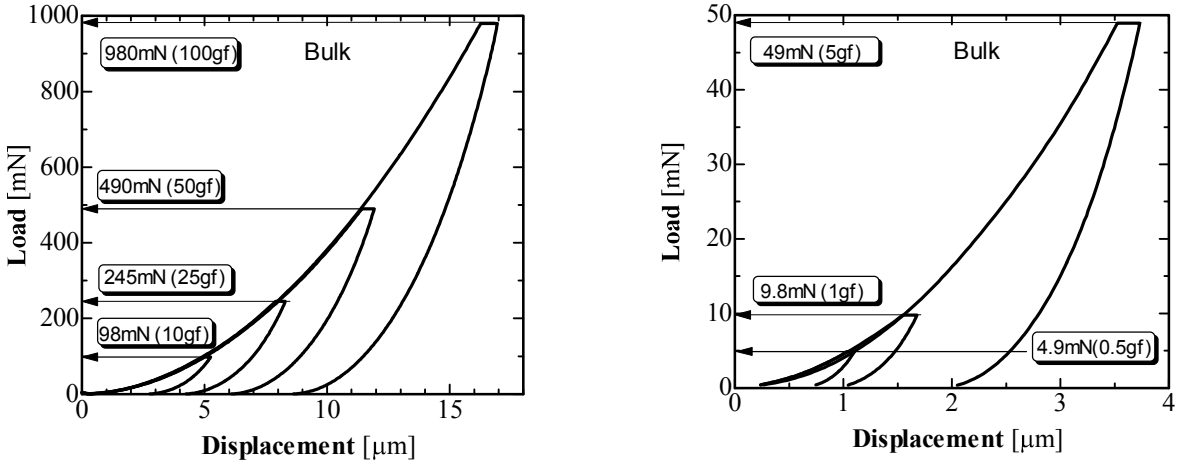

Fig.4 Experimental data of loading and unloading curves for bulk specimen

Table 2 Averages of the measured indentation depth δ_t and elastic recovery displacement δ_r for the BK7 specimen, the HMV500 specimen and bulk specimen

	BK7			HMV500			Bulk		
L_M [mN]	Avg. δ_t [nm]	Avg. δ_r [nm]	δ_r/δ_t	Avg. δ_t [nm]	Avg. δ_r [nm]	δ_r/δ_t	Avg. δ_t [nm]	Avg. δ_r [nm]	δ_r/δ_t
4.9	157	96.7	0.61	144	35.1	0.24	1099	450	0.41
9.8	241	136	0.57	212	55.0	0.26	1680	736	0.44
49	612	312	0.51	545	114	0.21	3726	1722	0.46
98	876	436	0.50	793	153	0.19	5223	2472	0.47
245	1420	700	0.49	1307	245	0.19	8295	4041	0.49
490	2046	986	0.48	1893	344	0.18	11915	5830	0.49
980	2930	1404	0.48	2679	479	0.18	16962	8361	0.49

Table 2 Averages of the measured indentation depth δ_t and elastic recovery displacement δ_r for the specimen to which two aluminum alloy plates were sticked with adhesive

Distance from bondline (μm)	BK7			
	L_M [mN]	Avg. δ_t [nm]	Avg. δ_r [nm]	δ_r/δ_t
10	0.98	437	-	-
20	4.9	1265	466	0.37
30	4.9	1182	466	0.39
40	4.9	1109	464	0.42
60	4.9	1201	480	0.40
80	4.9	1229	473	0.39
100	4.9	1202	521	0.43

3. EXPANDED PRACTICAL NANO-INDENTATION THEORY OF THE PYRAMID INDENTER

3.1 Testing machine calibration factor x and spring constant C of the tester

In the practical load range of the nano-indentation test with the pyramidal indenter, following expanded theoretical equations have been proposed [3].

For the quadrangular pyramidal indenter[Fig.8], the symbols in the next equations are as follows; L_M: load, δ_t : measured indentation depth, δ_r: measured elastic recovery displacement, x: testing machine calibration factor, C: spring constant of the tester, T_{Qua}: truncation of the indenter's round tip, β_{Qua}: the opposed face angle of the indenter, E_I, E_S, μ_I, μ_S: Young's moduli and Poisson's ratios of the indenter and specimen respectively, $F(E)_{IS}$ [=1/E*: E* is the reduced modulus, in the other paper[5]] : elastic parameter of the indenter and the specimen.

$F(E)_{IS}$ is defined as

$$F(E)_{IS}=(1-\mu_I^2)/E_I+(1-\mu_S^2)/E_S=I(E)+S(E) \quad (1)$$

The expanded theoretical formula of Young's modulus of the specimen E_S is as follows

$$E_S=\left(1-\mu_S^2\right)\Big/\left[\left(\frac{4}{3\sqrt{\pi}}\right)\frac{k_{0Qua}\cdot\delta_{tf}\cdot\delta_{rf}}{L_M}\left(1-x\frac{\delta_{rf}}{\delta_{tf}}\right)-I(E)\right] \quad (2)$$

$$\left.\begin{aligned}\delta_{tf}&=\delta_t-C\cdot L_M+T_{Tri}=\delta_t-\delta_E+T_{Tri}\\ \delta_{rf}&=\delta_r-C\cdot L_M=\delta_r-\delta_E\end{aligned}\right\} \quad (3)$$

δ_{tf} is the final corrected indentation depth, δ_{rf} is the final corrected elastic recovery displacement.[Fig.1]

$$k_{0(Qua)}=2\tan\left(\frac{\beta_{Qua}}{2}\right) \quad (4)$$

The equation of x is as follows,

$$x=\frac{\delta_{tf}\cdot\delta_{rf}-K_0\cdot L_M}{\delta_{rf}^2} \quad (5)$$

The coefficient K_0 is defined as

$$K_0=\frac{3\sqrt{\pi}\cdot F(E)_{IS}}{4\cdot k_{0Qua}}=\frac{\delta_{tf}\cdot\delta_{rf}}{L_M}\cdot\left(1-x\cdot\frac{\delta_{rf}}{\delta_{tf}}\right) \quad (6)$$

A schematic figure of the tip of the indenter is shown in Fig.5. In Fig.6, the schematic relationships between the load L and the displacement δ_t, δ_r, δ_{tf}, δ_{rf} are shown in Fig.7.

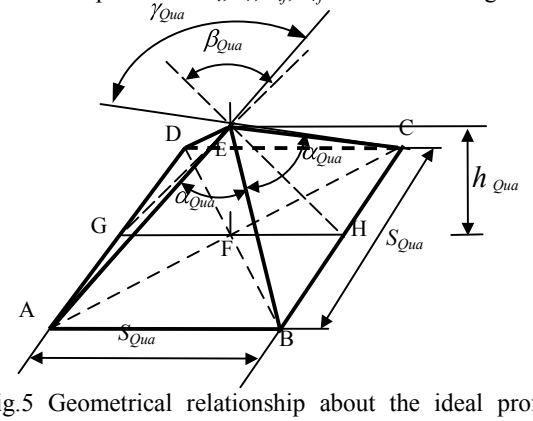

Fig.5 Geometrical relationship about the ideal profile quadrangular pyramidal indenter

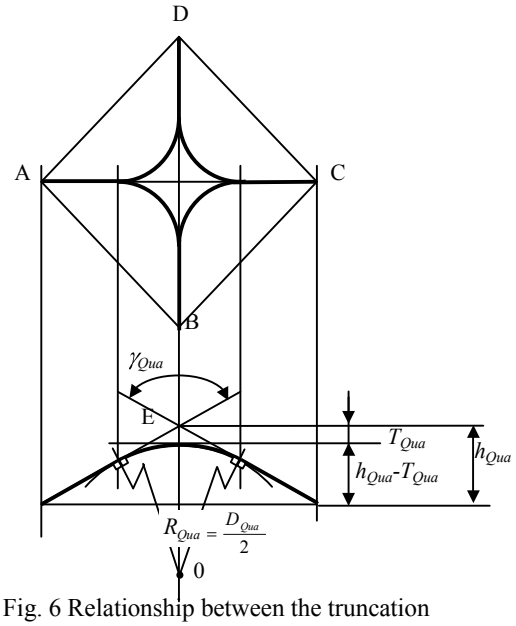

Fig. 6 Relationship between the truncation and the diameter of the round tip (R_{Qua} : Radius)

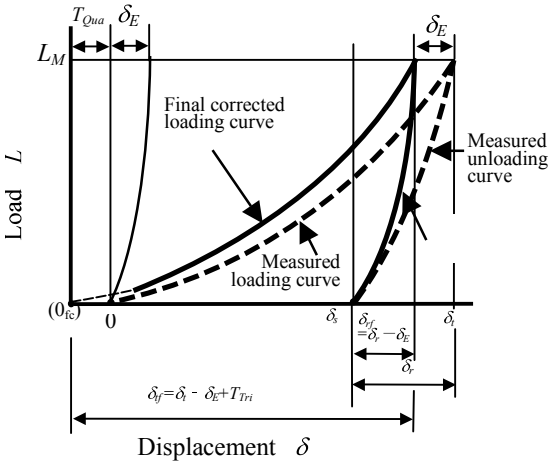

Fig.7 Schematic relationships between load L and displacement δ_t, δ_r, δ_{tf}, δ_{rf}

3.2 Hardness values during indentation

The hardness value using the triangular pyramid indenter at the final corrected indentation depth δ_{tf}, namely at the maximum indentation load L_M, is defined as $HI_{Berko.}$ in the former paper[3].

$$HI_{Berko.}=C_{Berko.}\times\frac{L_M}{\delta_{tf}^2} \quad (7)$$

The Vickers indenter (quadrangular pyramid indenter) is used in these experiments, so that the hardness value using the Vickers indenter is defined $HI_{Vick.}$ as follows.

$$HI_{Vick.}=0.0378\times\frac{L_M}{\delta_{tf}^2} \quad (8)$$

4 .APPLICATION TO THE EXPANDED PRACTICAL NANO-INDENTATION THEORY

4.1 Calculation of the testing machine calibration factor x and spring constant C of the tester

In order to determine the testing machine calibration factor x, the measured values of the same test load of the BK7 specimen and the HMV500 specimen: (L_M, δ_{t1}, δ_{r1}), (L_M, δ_{t2}, δ_{r2}), are used. Values of x are written as x_1 and x_2 in Eq.(9).

$$x = x_1 = \frac{(\delta_{t1} + T_{Tri} - \delta_E)\cdot(\delta_{r1} - \delta_E) - K_0 \cdot L_M}{(\delta_{r1} - \delta_E)^2}$$
$$= x_2 = \frac{(\delta_{t2} + T_{Tri} - \delta_E)\cdot(\delta_{r2} - \delta_E) - K_0 \cdot L_M}{(\delta_{r2} - \delta_E)^2} \quad (9)$$

When an arbitrary value of T_{Qua} is assumed and a value of δ_E is varied over the considered value range, the solution x at x_1=x_2 is obtained.

This procedure must be repeated using the combination in the different test load. Relationships between T_{Qua} and x in every combination at the same load are obtained. These lines obtained by this procedure are shown in Fig.11. Solution values of T_{Qua} and x are obtained from the intersection of the lines.

Therefore, the truncation T_{Qua}=60.6nm and testing machine calibration factor x=0.458 are obtained for the BK7 specimen and the HMV500 specimen.

Also, the spring constant C is given by T_{Qua} and x. Next quadratic equation is obtained from Eq.(6) and Eq.(3) by rearranging with respect to the elastic deformation δ_E(=$C\times L_M$).

$$\delta_E{}^2 + a_1 \cdot \delta_E + b_1 = 0 \quad (10)$$

Where, the coefficients a_1 and b_1 are as follows.

$$a_1 = \frac{(2x-1)\cdot\delta_r - \delta_t - T_{Qua}}{1-x} \quad (11)$$

$$b_1 = \frac{(\delta_t + T_{Qua} - x\cdot\delta_r)\cdot\delta_r - K_0 \cdot L_M}{1-x} \quad (12)$$

$$\delta_E = C \cdot L_M = \frac{1}{2}\left\{ -a_1 - \sqrt{a_1{}^2 - 4\cdot b_1} \right\} \quad (13)$$

Therefore, the spring constant C is obtained by these equations. As a result, C is changes by the load, and the elastic deformation of the tester δ_E is not linear. Then, δ_E =$C\times L_M$ is obtained by calculating each test loads.

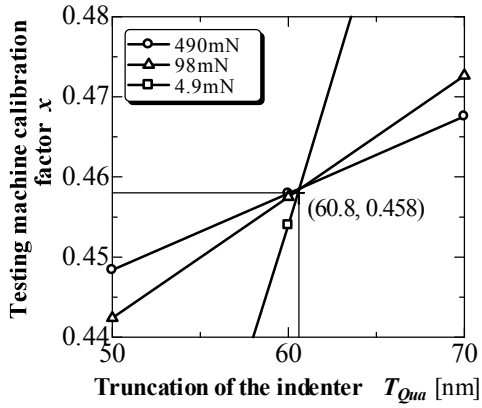

Fig.8 Relationships between the truncation T_{Qua} and the testing machine calibration factor x

5 .RESULTS AND DISCUSSIONS

5.1. Calculated Young's modulus

Using the testing machine calibration factor x, the truncation T_{Qua} at the tip of the indenter and the spring constant C of the tester, Young's moduli E_S of the specimens were calculated from Eq.(2). The mean value of results of the bulk specimen is equal to 2.33Gpa. However the results of the specimen to which two aluminum alloy plates were sticked with adhesive are shown in Fig.12.

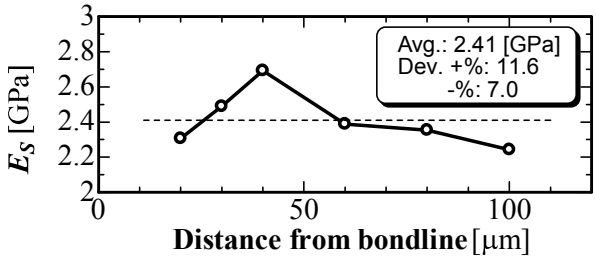

Fig.9 Relationships between distance from bondline and Young's modulus E_S

There is the remarkable peak value at the distance from bondline 40μm. In the case of the bulk specimen, there is a only difference of 7%. The mean value almost becomes the same in the case of the bulk specimen if the peak value is excluded. The data of less than displacement 0.4mN cannot be obtained for the specification of the tester. Therefore, the elastic recovery displacement δ_r is difficult to read from the experimental data. The calculation of Young's modulus E_S is impossible in 0.98mN at the distance from the bondline 10μm.

5.2. Calculated hardness value

The calculated hardness values $HI_{Vick.}$ during indentation by Eq.(8) for the specimen to which two aluminum alloy plates were sticked with adhesive is in Fig.13. The values of the bulk specimens are almost uniform. There is an only difference of 6%.

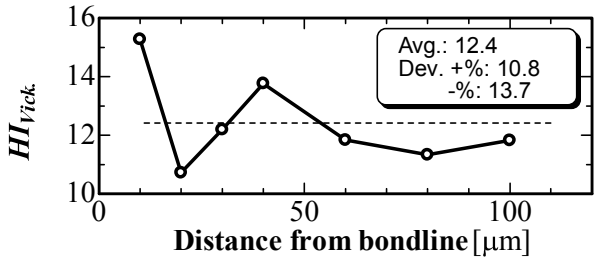

Fig.10 Relationships between distance from bondline and $HI_{Vick.}$

The influence of bondline edge effect (influence of adherend) is seen at the distance from bondline 10μm. However the change of a remarkable hardness value $HI_{Vick.}$ in the direction of depth is seen. In the range of the distance 60mm or more from the line, the hardness values are almost uniform.

3. CONCLUSION

(1) In order to evaluate the in situ mechanical properties of adhesives, nano-indentation testing is carried out for the calibration specimens and two kinds of the specimens of adhesive.

(2) The expanded nano-indentation theory proposed in the former paper applied to the test results and obtained the testing machine calibration factor x and the truncation of T_{Qua} at the tip of the indenter and the spring constant C of the tester.

(3) The hardness value $HI_{Vick.}$ during indentation at the final corrected indentation depth is defined as one of the material characteristic value.

(4) Young's moduli E_S and hardness values during indentation $HI_{Vick.}$ calculated for two kinds of the specimens of adhesive based on the expanded theory to obtain the distribution of local mechanical properties. Therefore, there is the change of remarkable mechanical properties near the bondline.

Acknowledgements

The authors wish to express their sincere thanks to prof. Tatsuya ISHIBASHI (Niigata University, Faculty of Engineering) for his constant encouragement and support. Also, the authors are grateful to President Shigeo KATAYAMA and Mr. Takao IMAI, Fischer Instruments JAPAN for their experimental help.

REFERENCES

[1] J.Bouchet, A.A Roche and E.Jacquelin "How do residual stress and interphase mechanical properties affect practical adhesion of epoxy diamine/metallic substrate systems?", *J.Adhesion Sci. Technol.*, vol.16, No.12,pp.1603-1623. 2002.

[2] L.Lilleheden "Mechanical properties of adhesives in situ and in bulk", *INT.J.ADHESION AND ADHESIVES.*, vol.14, No.1,pp.31-37. 1993.

[3] M.Fujitsuka, T,Ishibashi and M.Ohki, "Practical Nano-indentation Theory and Experiments of the Pyramidal Indenter(4th)", *J.Mater.Test.Res*, vol. 48, No.3 pp. 145-153, 2003.

[4] J.E.Field and R.H.Telling: Research Note, PCS Cavendish Laboratory .1999

[5] Pharr, Oliver & Brotzen :*J. Mater. Res.* : **7**, 613,1992

Author: Dr. Masyuki Fujituska, Precision and Intelligence Laboratory, Tokyo Institute of Technology, E-Mail: mfuji@pi.titech.ac.jp, R2-31 4259 Nagatsuta-cho, Midori-ku, Yokohama, 226-8503 JAPAN, Phone&Fax.: +81-45-924-5062